MEASUREMENT OF FREE SURFACE DEFORMATION BY REFLECTANCE-SCHLIEREN METHOD

Scheid B.[1](*), Kabov O.A.[2], Minetti C.[1], Colinet P.[1], Legros J.C.[1]

[1] Université Libre de Bruxelles, Microgravity Research Center, Brussels, Belgium.
[2] Institute of Thermophysics SB RAS, 630090, Novosibirsk, Russia.

ABSTRACT

The surface thermocapillary effect is studied for a thin liquid film falling on a vertical plate and locally heated, leading to the formation of a horizontal bump. A reflectance-schlieren method was developed to facilitate accurate measurement of the relative film thickness by measuring the slope of the surface. The experiments were performed for two non-evaporative ethyl alcohol aqueous solutions (10% and 25%). A fluid circulation system produced steady films at constant mass flux. Data are presented for film thickness profiles as function of the liquid Reynolds number and the heat flux density. The results show that the reflectance-Schlieren method is totally appropriate for high accuracy measurement and for a large range of surface deformation (up to 3 degrees). Extended analysis is presented for vertical rivulets appearing above a critical heat flux threshold for which the above-mentioned bump becomes unstable. As the deformations become bigger and the flow structure has to be considered in three-dimensions, recommendations are made in order to realise measurements under those new conditions.

1. INTRODUCTION

The processes in thin liquid film are widely used in various industries, for example in low pressure evaporators for concentration of food products or drugs. Marangoni effect, caused by non-uniformity of surface tension on a vapour/gas - liquid interface, at small Reynolds numbers is often the dominant mechanism for the occurrence of deformations of the film surface and can influence essentially heat transfer and crisis phenomenon. In the work of Kabov et *al.* [1, 2], a phenomenon of regular horseshoe-like structures was discovered and studied through experimentation and theory within a thin liquid layer approximation. At a threshold heat flux density, the flow becomes divided into vertical rivulets with specific wavelength and a thin film between them. Previously to the rivulets formation, a horizontally oriented liquid bump was observed. This paper deals with an experimental investigation of this bump, by determining the relative film thickness profile. This latter is obtained by an optical method measuring the one-dimension slope of the surface along the flow direction.

2. SCHLIEREN METHOD

2.1 Background

Preliminary tests [1] gave an idea of the order of magnitude of the surface slope to be measured, which turns around one degree. Practically, it means that system using coherent light (namely laser) with collimated beams is not suitable because out of the appropriate range (too small in this case). On the other hand, electro-mechanical probe, line projection or fluorescent imaging [3] do not provide easily the right resolution. An optical method working with incoherent lighting was used, namely the Schlieren. This method usually used for qualitative observations [4], was designed in order to measure surface deformations at a falling film surface. Other variations of the technique exist in a quantitative fashion [5, 6] but the main advantage of ours is that it can be easily used for a large range of slope.

2.2 Optical set-up

Here we describe a simple and practical quantitative schlieren method giving, without scanning, the slope in a particular direction, say $\partial h/\partial x$ as a function of the co-ordinate x in the same direction. The method is useful to probe steady as well as unsteady liquid surfaces.

Referring to the Figure 1, a *diffuser* and a *coding filter* for which their purpose will be explained later are placed before an incoherent *light source*. Plane waves generated by a *collimating lens* pass through a 50% *beam splitter* towards the *sampling surface* for which the slope will be measured. The collimated beam is then focalised by the *schlieren lens* in the *schlieren plane*. In this plane is placed a spatial filter so-called *schlieren stop*. Closely behind, a *camera lens* images the sampling surface on a *CCD camera*.

If the sampling surface is completely flat, the coding filter will be imaged in the schlieren plane, exactly centred on the optical axis as drawn on the Figure 1 by the continuous line. On the other hand, the image of a side point on the coding filter will be stopped by the schlieren stop as depicted by the dotted line. Nevertheless the image of the sampling surface won't be distorted as the schlieren stop is placed in the focal distance of the schlieren lens, namely the Fourier plane: only the intensity will be modulated in function of the surface slope by the mechanism explained in the following.

The deformation of the surface will deflect the incident collimated beam. To show how the orientation of a given element of the sampling surface can be determined from the brightness of its image, we must define the position and orientation of the element and draw the path followed by a light beam reflected by this element through the schlieren stop to the image plane. In this study, we will consider deformation in only one direction at a time (vertical or

horizontal). In this treatment, we shall recognise the following assumptions of the geometrical optics: - the reflected ray is in the plane formed by the incident ray and the normal, both projected on the effective direction; - the angle of reflection is equal to the angle of incidence.
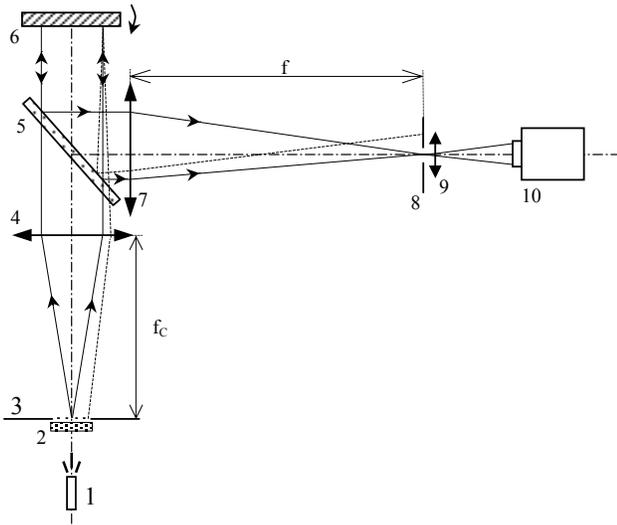
Figure 1: <u>*Reflectance-Schlieren set-up*</u>: *1-Light source, 2-Diffuser, 3-Coding filter, 4-Collimating lens, 5-Beam splitter, 6-Sampling surface, 7-Schlieren lens, 8-Schlieren stop, 9-Camera lens, 10-CCD camera.*

For the optical analysis, we can reduce the schlieren equipment to the portion of the system between schlieren lens and its focal plane and simplify the source as a simple pinhole and the stop as a knife-edge (Figure 2). For an element R on the sampling surface with an angle α with respect to the reference, the angle between the ray reflected by the point R and the optical axis is 2α. If the angle α were zero, the ray reflected by the surface element would pass through the point O_S, centre of the schlieren plane. If α is not zero the reflected beam will fall on a point R_S on the schlieren plane, at the distance ε from O_S.

Let f be the focal length of the schlieren lens. The relation between α and ε is

$$\varepsilon = f\tan(2\alpha) \approx f 2\alpha \qquad (1)$$

for small values of α (1% error for $\alpha = 5°$). If d is the width of the source and f_c the focal length of the collimating lens, the maximum value of ε can be expressed as

$$\varepsilon_{max} = \frac{f}{f_c}\frac{d}{2} \qquad (2)$$

Then, matching Eq.(1) and Eq.(2) we get

$$\alpha_{max} = \frac{d}{4f_c} \qquad (3)$$

It's interesting to note that α_{max} does not depend upon f. It is then the angle of the incident beam that contains the modulation feature of the system. It results that all the object

must be illuminated with a beam of incidence at least twice larger than the largest deflection to be measured. The factor two is due to reflection on the surface where deflection has to be measured: if the object surface is deflected by an angle α, the incident light beam will be reflected by an angle 2α.
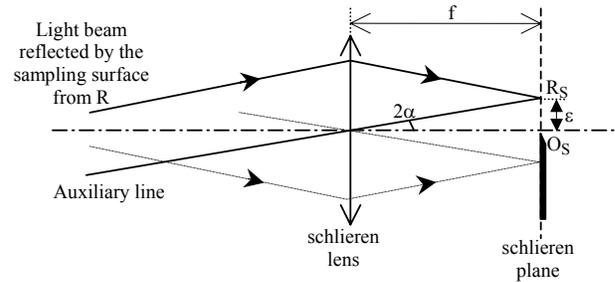

Figure 2: *Path of reflected beam*

Observing the Eq.(3), the size of the illuminated field on the sampling surface is limited by the diameter of the collimating lens. It means its f-number (ratio between the focal distance and the diameter, order of magnitude: 5) limits the parameter f_c. Concerning the parameter d it should be directly related to the diameter of the camera lens to avoid vignetting that would distort the linearity of the slope quantification.

2.3 Enhancement of the Schlieren method

It is naturally presumed in the foregoing that the light source itself produces constant brilliance over its surface. That implies the use of a diffuser as mentioned above. Furthermore, the deflected rays may still traverse the camera lens. This condition limits the maximum slope range available except if the incident light beam contains already the information about the slope in terms of intensity. That is the purpose of the use of a coding filter as a source instead of a simple pinhole. It consists of a grid of parallel bands with different optical density, coding then the light source into a spatially discrete variation of intensity as presented in the Figure 3.
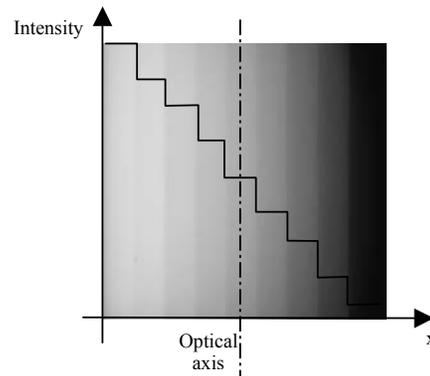
Figure 3: *Coding filter with intensity distribution*

In the Schlieren plane, the knife-edge is then replaced by a slit with exactly the same width than the image of one of the nine coding filter bands, and in the same orientation.

The filter is made in such a way that the variation of the band absorption is linear, providing the advantage of a linear slope codification. The principle of the typical schlieren can be reported for each band pairs. We see here a relevant way to increase the slope range by increasing the width of the coding filter as well as the number of bands. Actually, referring to the Eq.(3), we dropped the limitation on the parameter d.

Referring again to the Figure 1, if a global deformation of the sampling surface occurs for instance in the way indicated by the arrow next to the sampling surface, the light beam drawn in dotted line, this time, will be selected. As the intensity of the two different light beams presented is different, because coming from a different zone of the coding filter, the light intensity distribution in the image plane will be, as predicted, the result of a slope modulation.

2.4 Overlapping of the incident collimated beams

The incident angle of each beam coming towards the reflecting surface is function of where it is generated from the coding filter that modulates its light intensity. The problem here concerns the uniform overlapping of all those beams on the sampling surface. Actually, if we trace the beams from the two edge points of the filter, at the distance $d/2$ from the optical axis, we can define the effective observation area on the reflecting surface, reached uniformly by all the slope range coded in the incident light beam (Figure 4).

A remark must be done again about the uniformity of the light source. Only the placement of a uniform and strong diffuser before the coding filter allows us to consider the above scheme as realistic.
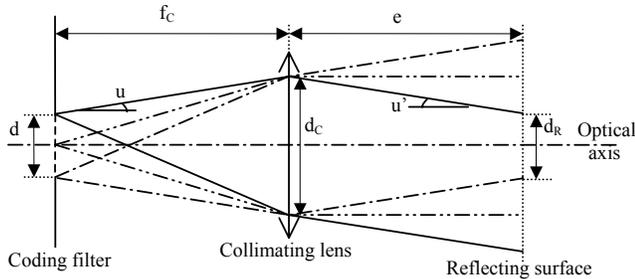
Figure 4: *Beam overlapping for effective observation area.*

Referring to the figure 4, we can write, being into the *paraxial region* (thin threadlike region about the optical axis which is so small that all the angles made by the rays may be set equal to their sinus and tangents) and with the *common sign convention* (the distances measured to the left of a reference point are negative; to the right, positive. The lens centre is commonly taken as convention. Moreover, the slope angles (u and u') are positive if the ray is rotated clock-wise to reach the axis, the light travelling from left to right),

$$u = \frac{d_c - d}{2 f_c} \tag{4}$$

$$u' = u - \frac{d_c}{2 f_c} \tag{5}$$

Let d_R be the size of the overlapping area and e the distance between the focal plane of the collimating system and the reflecting surface as shown on the Figure 4, we get

$$\frac{d_R}{2} = \frac{d_c}{2} + e u' \tag{6}$$

We obtain from (5) and (6),

$$d_R = d_c - \frac{d}{f_c} e \tag{7}$$

The distance e has to be as short as possible, observing Eq.(7), if we don't want to see the observation area d_R decreasing dramatically. Particularly since the slope range, following Eq.(3), has to be large.

3. INTERPRETATION OF THE SCHLIEREN IMAGE

3.1 Magnitude

To determine the magnitude of the imaging process, we define the position of a liquid surface element by the co-ordinates (x, z) on the plane of the undisturbed surface (on which the camera is focalised). The corresponding position of the element on the image plane is (x_i, z_i). It should be noted that the simple relation between these variables depends only upon the geometry of the disturbed sampling surface, the focal length and the position of the schlieren lens. Neither the nature of the schlieren stop nor the direction of incident and reflected light beam have any effect in absence of lens aberrations.

Let's use the simple law of geometrical optics with respect to the above-mentioned sign convention, i.e. *$1/s' - 1/s = 1/f$* where s' and s are respectively the distance of the image and the object taken positive from the lens position on the optical axis. The relative magnification is *$m = s'/s$*. Applied to our problem, we can determine the magnification M of the imaging process as being the product of the magnification produced by each lens. If f_i is the focal length of the camera lens and s the distance between the falling film and the schlieren lens, we get

$$M = \frac{f}{s + f} \cdot \frac{f_i}{f \left(\frac{s}{s + f} - 1 \right) + f_i} \tag{8}$$

Equation (8) informs us that the larger the distance s will be, the larger the magnification will be. This dependence (the two other parameters being fixed) is closely linear in the working range s [-150 mm; -450 mm] and it comes to the same consideration for f_i in the working range f_I [50mm; 200mm]. On the other hand the dependence of f on the magnification M is closely proportional.

To limit the vignetting problem of the camera lens, it is enough to certify that its f-number should be higher than the schlieren lens.

3.2   Brightness

Let h be the thickness of the liquid film as a function of perpendicular direction x and z, thus $h = h(x,z)$. Having one-dimensional system, we have two possibilities: - If the coding

filter is oriented vertically as shown in Figure 3, along *x*-axis, the brightness of each point will normally be proportional to the slope $\alpha(x)=\partial h/\partial x$; - If the coding filter is oriented horizontally, along *z*-axis, the brightness of each point will normally be proportional to the slope $\alpha(z)=\partial h/\partial z$.

Naturally, the coding filter has to be oriented following the direction along which we need to measure deformations. Moreover, the reason why the bands are designed so long appears clearly here. It is to allow some transverse deflection without influence on the image brightness.

In reality, the surface deformations are in 2 dimensions. But as explained just above, for our system, the ray deviations produced by the sampling surface are assumed to be contained in only one dimension, the vertical one, i.e. within the x-y plane (see Figure 6). The reflective angles with respect to the *y*-axis are given by $\alpha(x)$ and the transverse deviations $\alpha(z)$ are assumed to be zero. We have thus to take care to measure slope on vertical lines where this condition is valid. The same reasoning can be done for horizontal deformations, due to vertical rivulets, within the y-z plane with angle given by $\alpha(z)$. In this case $\alpha(x)$ is assumed to be zero and we have to take care to measure slope where this condition is valid.

4. THE PRACTICAL OPTICAL SYSTEM

4.1 Devices and image processing

Light from an arc 150 W Xenon lamp is expanded by diffuser into the coding filter and then collimated by the collimating system. This latter is constituted by two achromatic lenses with focal length equal to 310mm and diameter 80mm (f-number=3.8). The focal length is f_c=169mm and the effective diameter d_c=80mm. From Eq.(3) and with an effective coding filter width of *d*=20mm, the slope range is $\pm\alpha_{max}$=±1.7 degree. The distance between the collimating system and the surface is given by $e\approx$300mm and then the observation area by $d_R\approx$40mm according to Eq.(7).

Let's now determine the magnification of the image process. The distance between the liquid surface and the schlieren lens is about $s\approx$300mm. The schlieren lens is chosen achromatic with a large focal length equal to *f*=500mm and with a f-number=5. Finally, the camera lens is also achromatic. We performed experiments with two different focal lengths: f_i=50.8mm and f_i=100mm. For this latter we can calculate the magnification of the imaging process, according to the Eq.(8), equal to *M*=-0.217 and then a scale factor of 1:4.6. The dimension of the sensing area of the CCD camera (XC-75CE, monochrome video camera module using a CCD (Charge Coupled Device) solid state image sensor) being 6.5x4.8 mm² (*HxV*), the available area on the film surface is 29.9x22.1 mm² (for f_i=100mm). The measured one by imaging a test chart is 27.9x19.9 mm². The difference between them can be explained by the small f-number of the lens (=2.5) which induces image distortion.

The brightness (i.e. intensity) distribution is analogically sounded on the sensible area of the CCD camera (without gamma correction on the camera) and converted by a frame-grabber (512x512 pixels) into digital level coded on 8 bits. This codification provides a range of 256 grey levels. In the following, we will speak about grey level instead of light intensity for all concerning image processing. The frame-grabber is installed in a PC. The images are stored on a hard

disk in order to be post-processed. A monitor connected to the frame grabber allows us to visualise in real time the falling liquid film and to record video sequences on a S-VHS recorder.

The post-processing is realised by software fully developed for this study. This software allows to select a horizontal or vertical line on the image of the locally heated falling liquid film and provide immediately the intensity distribution along this line. The distribution is first compared to the reference one on the same line (corresponding to the falling liquid film without heating). Then only relative deformations are taken into account. According to a preliminary calibration, each grey level is related to a slope value thanks to a look-up table. This look-up table is determined during the calibration process. Then the numerical integration is applied on the curve to get a one-dimensional profile of the film thickness.

4.2 Calibration

The calibration of the system is of course the main step before performing experiments. It is the matter of correlating each grey level to a specific angle. To optimise the resolution, the light source power needs to be adjusted in a way that the whole slope range is coded by a maximum of grey levels. For that, the calibration needs to be done with the definitive configuration with reflection directly on the falling liquid film. The rotation of the optical set-up, or the falling liquid film set-up, being complex for good accuracy, the held solution was to fix the beam splitter on a rotation stage. The reading of its angle scale gives immediately the adequate slope. It leads to the same thing in the schlieren plane because turning the beam splitter has the effect to displace the source image (of the coding filter). The spatial filtering (selection) of the schlieren stop plays then exactly the same rule than for surface deformation. However, the image is logically translated from its reference position. To understand it, see the Figure 1 and imagine rotation of beam splitter around its symmetrical axis.

To avoid distortion of the calibration curve due to this artefact, we have to ensure on one hand that the diameters of the schlieren lens is large enough for avoiding vignetting and on the other hand that a large area around the observation area is also uniformly illuminated. It is filled if the effective diameter of the collimating system is large enough and if the diffuser is efficient enough. All those mentioned conditions were filled. To be convinced, a test was performed to compare the usual calibration curve made following our process with a calibration curve obtained by replacing the falling liquid film by a mirror fixed on a rotation stage. This latter configuration can be called "test" because closer than the experimental conditions. A reflective filter is chosen in a way to approach the reflection rate of the liquid film. The calibration curves are shown in the Figure 5. The result is conclusive excepted for the extremes where the slopes will be quite underestimated.

The usual calibration curve of the Figure 5 shows how non-linear the response of the camera is, however not strongly enough to be considered. Actually, the variation of the resolution is small thanks to a large grey level range. The mean resolution is evaluated about 1' which is more than enough taking into account the reading accuracy which can be overestimated to 2'.
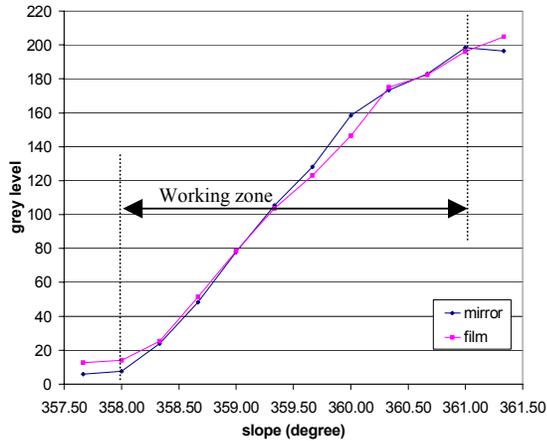
Figure 5: *Calibration curves: test curve with a mirror and usual one with the falling liquid film.*

Let's remark that the calibration curve is made by calculating the mean grey level on a complete image for each angle step of 1/3 degree. It seems to us that it is the easiest way for vanishing noise and ensuring reproducibility of the calibration process. For the same reason, the experimental set-up was placed in a dark room during measurements. Anyway a new calibration was made for each experiment for vanishing as well as possible uncertainty on light source power and variation of the ambient illumination. Nevertheless, all the obtained calibration curves were naturally similar.

The homogeneity of the grey level on all the image surface was done in order to ensure negligible effect of vignetting.
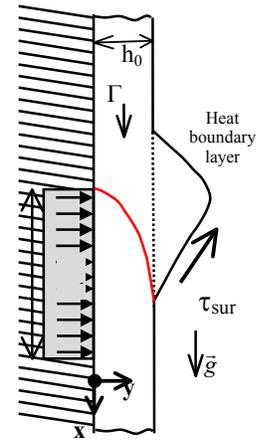
As we need information about the sign of the slope for numerical integration, the trick is to place the zero at the middle of the linear line at a grey level around 115. For that, one only has to adjust the rotation stage to the corresponding angle. Then a reference image will be immediately grabbed, giving the grey level for zero deformation and from which these will be measured.

A last remark can be done about the quality of the background surface on which falls the liquid film: - It has to be completely absorptive to avoid reflection on it and thus, effect of refraction along the path of the light beam inside the film. If not, we can have distortions of schlieren by reflection due to variation of refractive index by transmission; - Its flatness has to be better than 1μm to avoid preliminary deformation not caused by heating. However, this is not so critical as explained above thanks to the post-processing allowing to vanish this problem by doing relative measurement from reference image (without heating).

5. MEASUREMENT OF SURFACE DEFORMATIONS

In our recent work the problem of a liquid film essentially sub-cooled (up to saturation temperature) flowing under gravity along a vertical plate and heated locally was studied experimentally (Figure 6). The experiments were performed for two practically non-evaporative ethyl alcohol aqueous solutions (10% and 25%). Tests were carried out at atmospheric pressure with heat fluxes density q ranging from 0.2 to 6.6 W/cm², and film Reynolds numbers ranging from 0.09 to 2 (Re=Γ/μ, Γ - film flow rate per unit width, μ dynamic viscosity). The temperature of the initial liquid film was 20°C. The main attention was paid to the analysis of the development of a horizontal bump appearing at the liquid surface on the upper edge of the heater as depicted in the Figure 6.
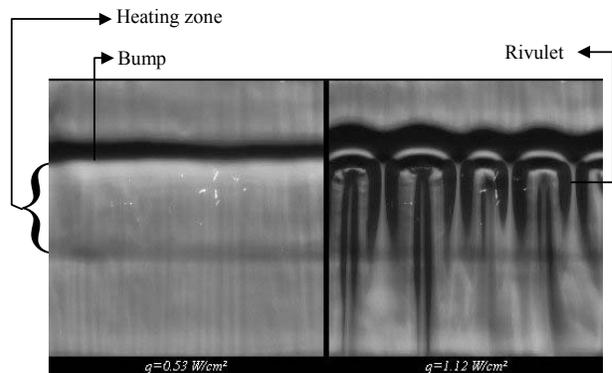
This observation gave rise to a new hypothesis being the possible appearance of a critical phenomenon. Indeed, this bump generated from a surface tension $\tau_{sur} = (\partial\sigma/\partial T)$ grad$T$ induced by the localised temperature gradient was thought to exist as soon as the heating begins. But for Reynolds number above 1, a minimum heat flux seems to be needed for inducing deformation.

The Figure 7 shows the Schlieren images of the front view of the falling film. On the left of this figure, the bump is putting in evidence by the technique and on the right, up to a critical heat flux, the rivulet structure is clearly installed. Both regime are steady.
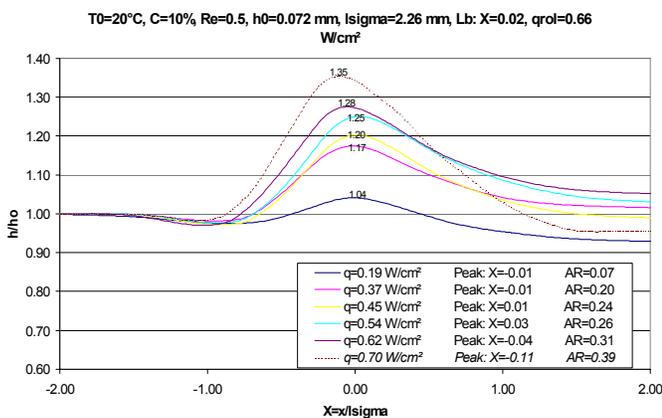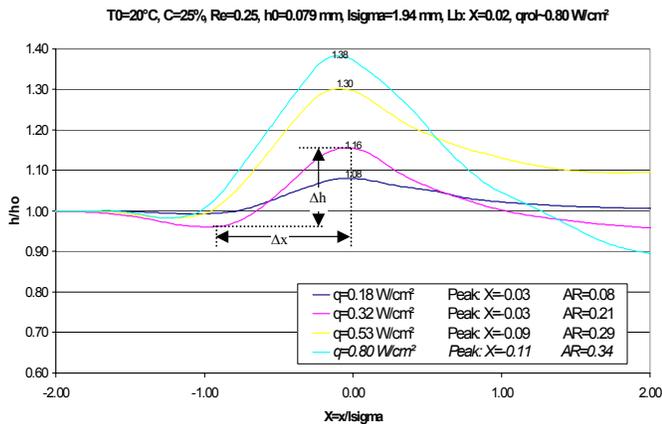
On the Figures 8 and 9 are presented the processed data of the film thickness profile. The rivulet structures occur once the maximum bump thickness have reached the range of 30%-40% of the initial thickness. That was foreseen in the work [1].

Figure 6: *side view of the falling liquid film locally heated, with an initial thickness h_0, and the horizontal bump at the upper edge of the heater. (q :heat flux, L :heater length)*

Figure 7: *Front view of the falling liquid film of 25% ethyl-alcohol solution locally heated. The Reynolds number is 0.25. The initial film thickness h_0 is 79 μm. The threshold of the heat flux density for the rivulet structure is at 0.80 W/cm².*

The reduction of the ratio h/h_0 below 1 is apparently connected to essential reduction of viscosity of a heated up liquid. For higher heat fluxes the influence of thermocapillary convection, which increases thickness of a film on a heater, is shown more strongly than effect of viscosity. However after

formation of structures on a part of the heater, the ratio h/h_0 becomes again smaller than one. That is caused by the three-dimensional nature of the flow structure implying that the major part of the liquid film flows down into the vertical

T0=20°C, C=25%, Re=0.25, h0=0.079 mm, lsigma=1.94 mm, Lb: X=0.02, qrol~0.80 W/cm²

T0=20°C, C=10%, Re=0.5, h0=0.072 mm, lsigma=2.26 mm, Lb: X=0.02, qrol=0.66 W/cm²

rivulets with a specific wavelength (Figure 7) and that between them, the film thickness can be extremely thin.

Figure 8 & 9: Mean vertical thickness profile measured by the Schlieren technique for two different concentrations: 10% and 25%. The position is scaled by the capillary length $l_{sigma}=(\sigma_0/\rho g)^{1/2}$, ($\sigma_0$ - surface tension coefficient, ρ - liquid density, g- gravitational acceleration) and the film thickness is scaled by its initial value calculated from the Nusselt theory. The upper edge of the heater is at the zero abscissa. The profile is shown at increasing of the average heat flux density on the heater with the corresponding peak position and the aspect ratio of the bump (AR=$\Delta h/\Delta X$). Above the chart are indicated in order the initial temperature, the ethyl alcohol concentration, the Reynolds number, the initial thickness, the capillary length, the position of the emergence point of the heat boundary layer L_b calculated by Gimbutis [7] (see Figure 6) and the critical heat flux density q_{rol} for the appearance of the rivulet structure.

The horizontal bump is slightly slicing upstream with the increasing of the heat flux. A 0.1-0.5 mm upstream shift of the peak bump was systematically observed during the transition between the stable bump and the rivulet structure. A 3% film thinning of the film thickness was also systematically observed at the base of the upstream side of the bump.

A new information about the shape of the bump and the bump displacement was obtained. It concerns at sharp change of the behaviour of the bump position versus the Reynolds number (Figure 10). This transition can be linked with a
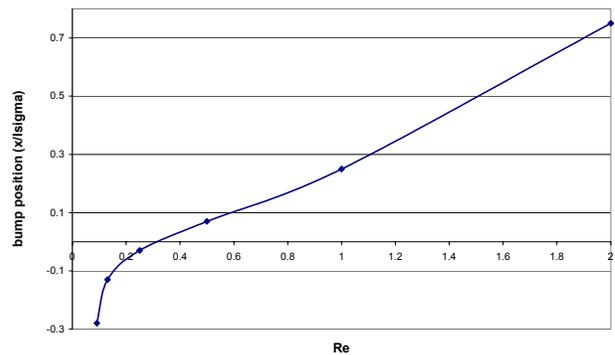
reverse thermocapillary flow at the interface, that was foreseen in the physical model of the regular structures formation proposed in the work [2].

Figure 10: Bump position (scaled with the capillary length) related to the upper edge of the heater versus the Reynolds number

6. CONCLUSIONS AND PERSPECTIVES

The Schlieren technique appears to be well appropriate for such kind of fluid physics experiment. The main qualities are the simplicity of its use, the high accuracy, and a large range of slope available. This latter reason was fully explored here and as in the application of the falling liquid film, the deformations can be even bigger when rivulet structure takes place, the range can be stretch even more. By adjusting the parameters, a range of 8 degrees can be easily reached with a resolution of 2.5'. On the other hand, the measurement of the deformation for the rivulet structures requests a two-dimensional measurement of the surface slope. That can be obtained with circular source and stop. Then, we can get a relative three-dimensional film thickness profile. Nevertheless, two consequences have to be pointed: under those new conditions, we loose the information about the sense of the slope and by increasing the dynamic slope range, we decrease the observation zone following the overlapping consideration mentioned above.

7. NOMENCLATURE

AR	aspect ratio, $\Delta h/\Delta x$
B	width of the heater, m
C	ethyl alcohol concentration by weigth, %
d	source diameter, m
d_c	collimating lens diameter, m
d_R	observation zone diameter, m
e	working distancr, m
f	focal length of the Schlieren lens, m
f_c	focal length of the collimating lens, m
f_i	focal length of the camera lens, m
g	gravitational acceleration, m/s^2
h	film thickness, m

h_0 initial film thickness, m
l_σ, l_{sigma} capillary length, m
L height of the heater , m
L_b length of the heat boundary layer region, m
m relative magnification, s'/s
M system magnification
q heat flux density, W/m^2
q_{rol} critical heat fluxes for rivulets, W/m^2
Re   film Reynolds number, dimensionless
s object distance from the lens, m
s' *image* distance from the lens, m
T surface temperature, °C
T_0 initial temperature of the falling film, °C
u incident angle, rad
u' output angle, rad
x, y liquid surface co-ordinates, m
x_i, y_i image co-ordinates, m

X, Y dimensionless co-ordinates, x/l_σ, y/h_0

Greek symbols

α surface slope, rad
α_{max} maximum measurable surface slope, rad
ε beam deviation on the Schlieren plane, m
Γ flow rate of liquid film, kg/(ms)
ρ liquid density, kg/m³
μ dynamic viscosity of the liquid, kg/(ms)
σ_0 surface tension, N/m
τ_{sur} shear stress on the liquid surface, N/m^2

8. REFERENCES

1. O.A. Kabov, I.V. Marchuk, A.V. Muzykantov, J.C. Legros, E. Istasse, and J.L. Dewandel, Regular Structures in Locally Heated Falling Liquid Films, *Proc. 2nd Int. Symp. on Two-Phase Flow Modelling and Experimentation*, G.P. Celata, P. Di. Marco and R.K. Shah, Eds., 23-25 May, Pisa, Italy, vol. 2.-pp. 1225-1233, 1999.

2. O.A. Kabov, Formation of Regular Structures in a Falling Liquid Film upon Local Heating, *Thermophysics and Aeromechanics*, vol. 5, No.1, pp. 547-551, 1998.

3. M. F. G. Johnson, R. A. Schluter, M. J. Miksis and S. G. Bankhoff, Experimental Study of Rivulet Formation on an Inclined Plate by Fluorescent Imaging, *J. Fluid Mech.,* vol. 394, pp. 339-354, 1999.

4. A. Okhotsimskii and M. Hozawa, Schlieren Visualisation of Natural Convection in Binary Gas-Liquid Systems, *Chemical Engineering Science*, vol. 53, No. 14, pp. 2547-2573, 1998.

5. L. Thomas, R. Gratton, B. Marino, S. Betelu, J. Diez and J. Simon, Measurement of the Slope of an Unsteady Liquid Surface Along a Line by an Anamorphic Schlieren System, *Meas. Sci. Technol.*, vol. 7, pp. 1134-1139, 1996.

6. H. Önder Özbelge, E N Lightfoot and E E Miller, Reflectance-Schlieren Technique for Measurement of Free Liquid Surface Perturbations, *J. Phys. E.: Sci. Instrum.*, vol. 14, pp. 1981.

7. I. Gimbutis, *Heat Transfer to a Falling Fluid Film*, Mosklas, Vilnius, 1988.